Beaked whale (*Mesoplodon densirostris*) passive acoustic detection in increasing ambient noise

Jessica Ward,[a] Susan Jarvis, David Moretti, Ronald Morrissey, and Nancy DiMarzio
Naval Undersea Warfare Center, Division Newport, 1176 Howell Street, Newport, Rhode Island

Mark Johnson and Peter Tyack
Biology Department, Woods Hole Oceanographic Institution, Woods Hole, Massachusetts 02543

Len Thomas and Tiago Marques
Center for Research into Ecological and Environmental Modelling, The Observatory, University of St. Andrews, St. Andrews, KY16 9LZ, Scotland

(Received 6 May 2010; revised 22 November 2010; accepted 29 November 2010)

Passive acoustic detection is being increasingly used to monitor visually cryptic cetaceans such as Blainville's beaked whales (*Mesoplodon densirostris*) that may be especially sensitive to underwater sound. The efficacy of passive acoustic detection is traditionally characterized by the probability of detecting the animal's sound emissions as a function of signal-to-noise ratio. The probability of detection can be predicted using accepted, but not necessarily accurate, models of the underwater acoustic environment. Recent field studies combining far-field hydrophone arrays with on-animal acoustic recording tags have yielded the location and time of each sound emission from tagged animals, enabling *in-situ* measurements of the probability of detection. However, tagging studies can only take place in calm seas and so do not reflect the full range of ambient noise conditions under which passive acoustic detection may be used. Increased surface-generated noise from wind and wave interaction degrades the signal-to-noise ratio of animal sound receptions at a given distance leading to a reduction in probability of detection. This paper presents a case study simulating the effect of increasing ambient noise on detection of *M. densirostris* foraging clicks recorded from a tagged whale swimming in the vicinity of a deep-water, bottom-mounted hydrophone array.
 [DOI: 10.1121/1.3531844]

PACS number(s): 43.30.Sf [WWA] Pages: 662–669

I. INTRODUCTION

Passive acoustic detection is used to monitor Blainville's beaked whales (*Mesoplodon densirostris*) on Navy undersea ranges. Typically, monitoring on the ranges involves automated detection of *M. densirostris* sound emissions received at deep-water, bottom-mounted hydrophones. The ability to detect *M. densirostris* within a certain geographic area, characterized by the probability of detection as a function of slant range from the animal to the sensor, is of particular importance to monitoring. The probability of detection versus range can be estimated theoretically using mathematical models of animal source characteristics, transmission loss (TL), ambient noise, signal-to-noise ratio (SNR), and animal movement. Zimmer *et al.* (2008) used this approach to predict Cuvier's beaked whale (*Ziphius cavirostris*) detection ranges at near-surface hydrophones. Results from such models are often incorporated into environmental compliance documentation, permit applications, and test plans without later *in-situ* validation.

The effectiveness of passive acoustic monitoring depends on the ability to identify a given animal sound in the presence of ambient noise and other sources of noise. Detection effectiveness is often characterized by the probability of detection, *Pd*, and the probability of false alarm, *Pfa*, in relation to the SNR. Here we approximate SNR by the power ratio of the sound of interest combined with noise to the noise alone. The *Pd* is the probability that a received animal sound exceeds the receiver threshold (RT), a design parameter. The *Pfa* is the probability that a noise peak exceeds the RT in the absence of an animal sound. The RT is usually chosen to maximize *Pd* for a given acceptable *Pfa* (Lurton, 2002). The SNR depends on the acoustic characteristics of the source (whale) and receiver (hydrophone), the orientation of the whale to the hydrophone(s), and the acoustic environment in the area of the source and receiver (Tyack *et al.*, 2006a; Zimmer *et al.*, 2008). *Pd* and *Pfa* depend on the SNR and on the hardware and software of the detector. This paper establishes a baseline *Pd* for *M. densirostris* foraging clicks in the Tongue of the Ocean (TOTO), Bahamas, and evaluates the effect of increasing surface-generated ambient noise on the *Pd* using a theoretical solution and simulated data.

Deep diving *M. densirostris* typically have an approximately 140 min dive cycle consisting of a single deep foraging dive followed by several shallow dives (Tyack *et al.*, 2006b). Foraging clicks are only produced during deep dives and tend to occur in 15–60 s long trains terminated by a buzz indicating a prey capture attempt (Johnson *et al.*, 2004; Madsen *et al.*, 2005). Clicking occurs for about 20–30 min per dive (Madsen *et al.*, 2005; Tyack *et al.*, 2006b). The foraging

[a]Author to whom correspondence should be addressed. Electronic mail: jessica.ward@navy.mil

clicks are a broadband high-frequency modulated upsweep [−10 dB bandwidth (BW) from 26 to 51 kHz] approximately 300 μs long with a mean interclick interval of 0.4 s (Zimmer *et al.*, 2005a; Johnson *et al.*, 2006). During an average foraging dive, a single whale may produce 5000 foraging clicks and some 10 000 buzz clicks (Madsen *et al.*, 2005). Foraging clicks, as opposed to buzz clicks, are the focus of this study due to their significantly higher source level (SL), regular interclick interval, and fairly continuous production during deep dives.

Previous studies of *Pd* for another beaked whale species, *Z. cavirostris*, have relied on theoretical assumptions about the ambient noise environment, TL, and source characteristics (Tyack, 2006a; Zimmer *et al.*, 2008). *In-situ* validation of *Pd* is difficult to accomplish since both the range from the whale to a receiver must be known as well as the number of clicks emitted by the whale at that range. Acoustic recording tags, such as the DTag (Johnson and Tyack, 2003), provide a reliable set of click emission times which, in combination with far-field recording and tracking hydrophones, can be used to estimate *Pd*. However, beaked whales can usually only be located and approached for tagging in low sea-state conditions. Analysis of data taken under these conditions potentially results in higher SNRs and greater *Pd* values at a given range than would be expected at higher sea-states with increased surface-generated ambient noise. Given the importance of accurate estimates of *M. densirostris Pd* for passive acoustic monitoring, we present here a case study comparing theoretical to measured results using bottom-mounted hydrophones at TOTO. To provide an estimate of *M. densirostris Pd* over a full range of weather conditions, we first characterize the ambient noise environment using daily ambient noise spectra collected on two hydrophones over an approximately 1 yr period. Using these spectra, we simulate higher sea-state/lower SNR conditions by adding synthetic ambient noise to low-noise hydrophone recordings of clicks from a tagged whale at known ranges. The resulting probability of detection estimates for *M. densirostris* foraging clicks as a function of SNR and range are valuable for designing effective acoustic monitoring and survey efforts for this species.

II. METHODS

A. Case study scenario

This study uses data collected during the 2007 Behavioral Response Study (BRS) in the TOTO, Bahamas (Boyd *et al.*, 2007). On September 5, acoustic recording tags (DTags, Johnson and Tyack, 2003) were placed on two whales in a group consisting of one adult male and two adult female *M. densirostris*. Three of four deep foraging dives recorded by the tag on the adult male are used in the current analysis. These dives had the greatest number of detected clicks with georeferenced dive tracks. The DTag records stereo audio at a sampling rate of 192 kHz per channel simultaneously, with an audio sensitivity of −171 dB re V/μPa. Analysis of the DTag audio data provides a time of emission (TOE) for each click on the tagged whale in terms of the tag clock. The DTag also records accelerometer, magnetometer, and pressure sensors at a sampling rate of 50 Hz per channel. These measurements are decimated and processed using the methods described in Johnson and Tyack (2003) resulting in pitch, roll, heading, and depth data at 5 Hz sampling rate. Heading is defined as the true heading corrected for magnetic declination angle and has a range of –180° to 180°. Pitch is positive for a nose-upward tilt and is restricted to a –90° to 90° range. Roll indicates rotation about the longitudinal axis of the animal and can be between –180° and 180°.

Prior to, and throughout the tag attachment to the whale, audio data were recorded from 82 bottom-mounted hydrophones in the Atlantic Undersea Test and Evaluation Center (AUTEC) tracking range (Moretti *et al.*, 2006). The hydrophones are mounted 4–5 m off the sea floor. The frequency-dependent receive beam pattern of these hydrophones transitions from roughly hemispherical at low frequency to become increasingly flattened vertically at higher frequencies within the range of *M. densirostris* sound emissions (e.g., greater than 24 kHz) (Maripro, 2002). The measured frequency-dependent horizontal and vertical hydrophone receiver beam pattern was used for all calculations in this study. The recordings were made using multiple Alesis HD24 digital recorders sampling at 96 kHz. Each Alesis HD24 can record up to 12-channels of data with one channel assigned to record an IRIG-B modulated time signal code. This study uses data from a subset of five of the 82 hydrophones that were in the vicinity of the tagged whale (Fig. 1). These hydrophones had a mean depth of 1630 m and a usable BW of 50 Hz to approximately 48 kHz when digitized at the 96 kHz sampling rate.

Hydrophone signals were processed using a fast Fourier transform (FFT) based energy detector. A 2048 point FFT with 50% overlap was used, resulting in a per-bin frequency resolution of 46.875 Hz and a time resolution of 10.67 ms. The magnitude of each bin of the FFT is compared to the noise varying threshold (NVT) for that bin (Ward *et al.*, 2008b). The resulting "detection spectrum" is a binary representation of detection (1) or no detection (0) information per bin. A detection is reported if any of the bins have passed

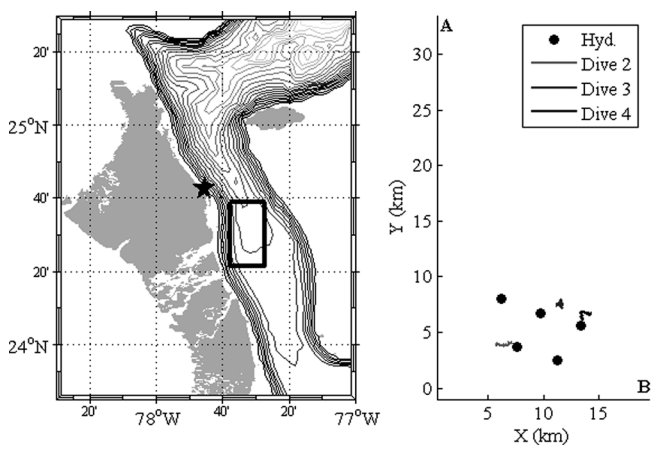

FIG. 1. Details of the geographical location of the field work. Left panel presents the location of the study area in the TOTO, offshore Andros Island, Bahamas. Black star indicates location of weather station. Right panel shows hydrophones A and B used for ambient noise measurement, as well as the five hydrophone array used to assess *Pd* (black circles), and the location of whale dive tracks.

the threshold and the binary FFT results are then archived to file.

B. Theoretical probability of detection

In a constant false alarm rate detector such as the one described here, the probability of detection can be characterized as the likelihood that the SNR of a processed signal exceeds the RT (Lurton, 2002). RT (dB) is defined as a function of the Neyman–Pearson hypothesis test of *Pfa* (Lurton, 2002),

$$\mathrm{RT} = 10\log(-2\ \ln(Pfa)). \tag{1}$$

The detector was configured for a *Pfa* of 0.214, a setting determined to provide optimal output to the M3R spectrogram displays and click classifier used for real-time monitoring (Ward *et al.*, 2008b). This corresponds to a RT of approximately 5 using Eq. (1).

The sonar equation provides a simplified means for predicting probability of detection as a function of range. For passive sonar, SNR (dB) is defined as (Lurton, 2002)

$$\mathrm{SNR} = \mathrm{SL} - \mathrm{TL} - \mathrm{NL} + \mathrm{DL} + 10\log\ \mathrm{BW} + \mathrm{PG}, \tag{2}$$

where SL is the source level of the whale ($\mathrm{dB_{rms}}$ re 1 μPa at 1 m) along the maximum output axis, TL is the one-way transmission loss (dB), NL is the noise level (dB re 1 $\mu\mathrm{Pa}/\sqrt{\mathrm{Hz}}$) at the receiver, directivity loss (DL) is the off-axis attenuation of the SL due to the transmission beam pattern of the whale (dB), BW is the processing bandwidth (Hz), and PG is the processing gain of the system (dB). The SL for *M. densirostris* is estimated to be 200 $\mathrm{dB_{rms97}}$ re 1 μPa at 1 m with an approximately 11° (−3 dB) beam width (Ward *et al.*, 2008a). The root mean square (rms97) level is calculated using the 97% energy duration of the click, with the window onset defined as the time at which 1.5% of the signal energy is reached and the window end time defined as the time at which 98.5% of the energy is reached (Madsen and Wahlberg, 2007).

TL is usually modeled using spherical spreading as a function of range, R (m), corrected for frequency-dependent absorption, α (dB/km),

$$\mathrm{TL} = 20\log_{10} R + (\alpha R/1000). \tag{3}$$

While negligible at lower frequencies, absorption becomes a significant factor at higher frequencies. Here we compare (3) to a more complex two-dimensional Gaussian eigenray model (Weinberg and Keenan, 1996). This two-dimensional model incorporates an estimate of the *M. densirostris* vertical beam pattern, as well as its SL and pointing angle (i.e., pitch angle in a 2-D model). The model uses a sound velocity profile (SVP) taken using an expendable bathythermograph on September 5, 2007, 1757 UTC at 77° 23′ 30″ W longitude, 24° 18′ 54″ N latitude. The SVP indicates a downward refracting environment for the 500–1200 m depths at which *M. densirostris* typically emit sound (Tyack *et al.*, 2006b).

Deep-water, open ocean ambient noise in the frequency range of *M. densirostris* clicks generally consists of three primary components: sea surface-generated noise, thermal noise, and volume generated noise. Ambient noise above 1 kHz and below 100 kHz is primarily caused by wind generated phenomena at the sea surface such as bursting clouds of air bubbles and breaking waves (Lurton, 2002). The ambient noise spectrum at the sea surface can be modeled as a function of frequency, f, as (Kurahashi and Gratta, 2008; Short, 2005)

$$\mathrm{NL_{surf}} = 10\log_{10}\left(f^{-5/3}\right) + 94.5\ \mathrm{dB\ re\ 1\ \mu Pa}/\sqrt{\mathrm{Hz}} \quad \text{for} \quad f = 1 - 40\ \mathrm{kHz}. \tag{4}$$

Surface-generated noise at higher sea-states is modeled by adding a correction factor, NL_{ss}, equal to 30 $\log_{10}(n_s + 1)$, where n_s is the sea-state (Short, 2005). Due to increased attenuation of the higher frequency noise components, this result is then corrected for the hydrophone depth using (Lurton, 2002)

$$\mathrm{NL_{depth}} = -\alpha h - 10\log_{10}\left(1 + \frac{\beta h}{2}\right) \tag{5}$$

where $\beta = \alpha/4343$, α is the absorption, as defined above, h = hydrophone depth (m) and f = frequency (Hz).

The resulting model of sea surface-generated noise becomes a function of frequency, sea-state, and depth,

$$\mathrm{NL}(f, n_s, h) = \mathrm{NL_{surf}} + \mathrm{NL}_{ss} + \mathrm{NL_{depth}}\ \mathrm{dB\ re\ 1\ \mu Pa}/\sqrt{\mathrm{Hz}}. \tag{6}$$

At the higher frequencies in this study, thermal noise also begins to increase the ambient NL and can be modeled by (Lurton, 2002)

$$\mathrm{NL_{thermal}} = -75 + 20\log f, \mathrm{dB\ re\ 1\ \mu Pa}/\sqrt{\mathrm{Hz}}. \tag{7}$$

The total ambient NL is the sum of the contributions of the sea surface-generated and thermal ambient NLs. Anthropogenic noise is not included in the simulated noise model as it is typically of short duration in the study area, consisting of fishing and military vessels transiting through the study area.

C. Empirical ambient noise

This study uses measured ambient noise spectra recorded approximately daily from October 2007 to September 2008 on hydrophones at 1560 m and 1580 m water depth (labeled A and B, respectively in Fig. 1). Ambient noise measurements were made using a spectrum analyzer set to calculate the rms average power over 100 measurements with a hanning windowed, 2048 point, no overlap FFT and a 131 072 Hz sampling rate. The power spectrum level was corrected by the system gain to arrive at the ambient noise spectrum level in dB re 1 $\mu\mathrm{Pa}/\sqrt{\mathrm{Hz}}$ (Maripro, 2002). Wind speed and direction were recorded at 10 min intervals from a weather station located on the AUTEC harbor jetty (Fig. 1).

D. Addition of colored noise

The surface-generated component of ambient noise depends primarily on the sea-state which is itself a function of the wind speed. To simulate the effects of increasing surface-generated ambient noise on *Pd*, synthetic ocean noise was generated and scaled to correspond to the average NL that would be observed at wind speeds of 11 and 21 knots (5.7 and 10.8 m/s) corresponding to low sea-state 3 and high sea-state 4, respectively. The synthetic ambient noise was created by filtering white Gaussian noise (generated in MATLAB version 7 with a cycle length of 2^{64} samples) using a finite impulse response filter whose coefficients were determined from the year-long ambient measurements (Jarvis, 1993). This noise was then added to low-noise recordings made during the tagging study to produce a low SNR signal for detector evaluation. The combined signal was stored as a wav-format file for processing through the Marine Mammal Monitoring on Navy Ranges (M3R) detection software toolset (Morrissey *et al.*, 2006).

The simulation was repeated at each test NL using the sound recorded from each of five hydrophones during the three dives performed by the tagged whale (Table I). During this time, the slant range of the whale from the hydrophones varied between 1 and 6 km with a gap at ranges between 3.2 and 4 km. The minimum slant range of 1 km in the data set is close to the minimum possible range of 800 m between the foraging depth of the whale at approximately 800 m and the 1600 m depth of the hydrophones.

E. Measured probability of detection

The raw (low noise) and treated sound files were processed through the FFT detector described previously. As the sound files contain clicks from multiple animals including the tagged whale, the resulting detections were examined to determine the proportion of the tagged whale's clicks that were detected. To do this, detections were correlated with the DTag click TOE using a comb sieve (Ward, 2002). The comb sieve has been found to be an effective means for associating patterns of detections among hydrophones for sperm whales (*Physeter macrocephalus*). A fundamental assumption is that each animal exhibits its own unique pattern of interclick intervals. In this procedure, the unique pattern of click emission times recorded by the DTag is used as a template which is correlated against the clicks detected on the surrounding hydrophones. For the untreated sound files, this analysis results in a set of time difference of arrivals (TDOA) between the DTag and each hydrophone on which the click was detected. The precise location of the whale for each click is obtained when TDOAs are measured on at least three hydrophones within the array (Ward *et al.*, 2008b; Ward, 2002). Given these locations, the orientation of the whale to the hydrophone is calculated for each click by transforming the pitch, roll, and heading recorded by the DTag into the azimuth and elevation angle of the hydrophone relative to the whale's longitudinal axis (Zimmer *et al.*, 2005b; Zimmer *et al.*, 2008).

While the presentation of *Pd* as a function of range enables a practical understanding of the ability to detect *M. densirostris* clicks for monitoring, a more traditional presentation is *Pd* as a function of SNR. To obtain the SNR for each detected click in this study, a 64 ms sound sample (i.e., three times the 21.3 ms span of the FFT detector window) was extracted around each detection. The entire click and noise sample was high-pass filtered at 15 kHz. The SNR was then calculated using the rms 97% energy criteria on a 1 ms sample centered on the envelope peak of the click and on a noise sample preceding the click.

A detection model of *Pd* as a function of SNR and range, respectively, was fit using a generalized linear model (GLM) with a binomial response and a logistic link function (McCullagh and Nelder, 1997). Confidence intervals for *Pd* as a function of SNR were estimated by bootstrapping observations (1000 bootstrap samples, resampling clicks). Due to the narrow forward-directed beam of *M. densirostris* (Ward *et al.*, 2008a), the probability of a click being detected decreases with increasing off-axis receiving angle. To better understand the effect on *Pd*, separate GLMs were created for clicks that were deduced to be on-axis versus off-axis, given the tagged whale's instantaneous orientation with respect to the receiving hydrophone. Clicks were considered on-axis when the sight-line to the receiving hydrophone was within ± 10 of the longitudinal axis of the whale, while angles outside of this range were considered off-axis. The 20° on-axis span is approximately 50% greater than the estimated beam width of 11° to account for uncertainty in the orientation of the whale relative to the hydrophone. As with other whales, *M. densirostris* may turn their head from side-to-side while echolocating to extend their search volume (Johnson *et al.*, 2006). The tag, being located posterior of the atlas vertebra would not track this movement leading to uncertainty in the axis of the acoustic beam in relation to the swimming direction of the animal (Rasmussen *et al.*, 2004; Johnson *et al.*, 2009).

TABLE I. Hydrophone recordings evaluated.

Dive	Duration (min)	Clicks recorded by DTag	Wind speed (m/s) mean (min–max)	Hyd.	Number of clicks detected	Slant range (m) (min–max)
2	40.3	6246	4.0 (3.3–4.5)	65	470	4220 (4077–4374)
				66	505	4400 (3857–5042)
				73	3711	1410 (1041–2169)
				74	309	5056 (4512–5834)
3	36.8	5718	3.9 (2.6–4.7)	66	2453	2089 (1857–2312)
				67	1665	2743 (2441–3175)
4	42.3	6299	3.5 (3.2–3.8)	67	2007	1340 (1033–1735)

III. RESULTS

A. Theoretical probability of detection

The clicks used in this study (i.e., those detected in the far-field recordings without added noise) are characterized by a mean whale pitch of 2.5° downward [coefficient of variation (CV) = 17%, where CV is the standard deviation/estimate, $n = 9305$] and mean whale depth of 800 m (CV = 12%). The peak frequency of on-axis clicks received on the hydrophones varies from 42 kHz at 1000 m range to 26 kHz at 5500 m range due to absorption of the high-frequency content of the clicks. The mean peak frequency of on-axis clicks detected over all ranges is approximately 30 kHz (CV 14%). An example of two-dimensional Gaussian eigenray model (Weinberg and Keenan, 1996) TL prediction is given in Fig. 2 for sound emitted by a whale at the mean depth and pitch angle showing that the main lobe of the beam pattern will be received at approximately 5600 m range for a hydrophone at 1630 m water depth.

The absorption coefficient (α) at 30 kHz is 6 dB/km using the Francois–Garrison equation (Lurton, 2002). Using this value, the predicted ambient NL at 30 kHz from Eqs. (4) through (7) is 15 dB re 1 μPa/$\sqrt{\text{Hz}}$ depth averaged between the whale and hydrophone (Fig. 3) (Lurton, 2002). To account for the decreased hydrophone sensitivity at 30 kHz in the vertical direction, PG is set to –11 dB. The BW of *M. densirostris* clicks received on the hydrophones is 24 kHz. For an RT of 5, Eq. (2) results in a maximum detection range of approximately 7.8 km using both the spherical spreading TL model and the eigenray TL model (cf. results for eigenray model for this scenario displayed in Figs. 2 and 4). However there are significant differences in the predicted received SNR between the two TL models at ranges less than 8 km. The spherical model, which assumes an omnidirectional source, overestimates the likelihood of detecting off-axis clicks, whereas the eigenray model more accurately simulates the highly directional nature of *M. densirostris* clicks.

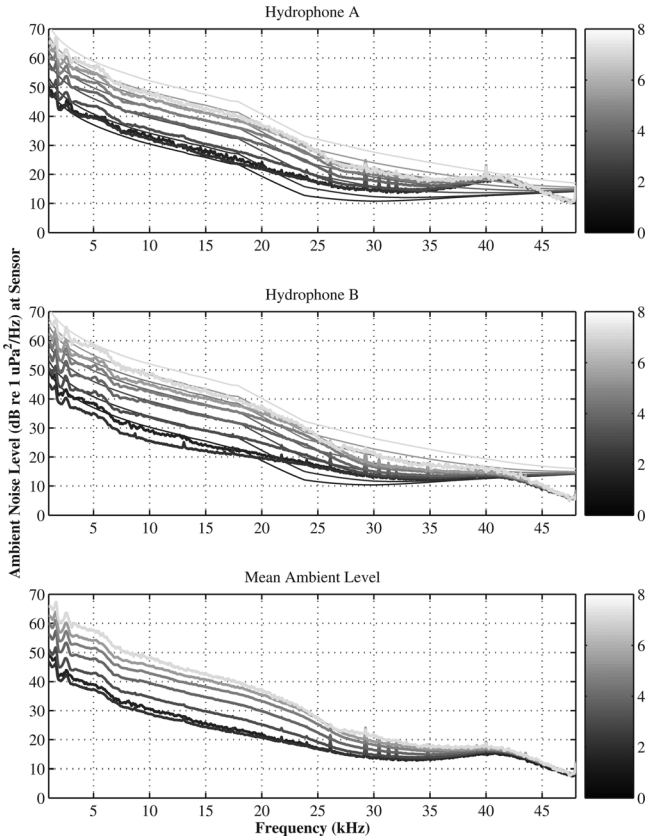

FIG. 3. Modeled versus measured ambient noise as a function of sea-state (color bar) for hydrophones A and B and the combined mean ambient NL (note: thin lines are modeled using Eqs. (4) through (7), thick lines are averaged measured data for sea-states 0.5, 1, 2, 3, 4, 5, 6, and 7.

B. Empirical ambient noise

Ambient noise varies spatially and temporally over the study area, depending on weather conditions, hydrophone depth, and proximity to noise producing features. Hydrophone A has a higher ambient noise spectrum than hydrophone B (Fig. 3, top and middle, respectively), perhaps due

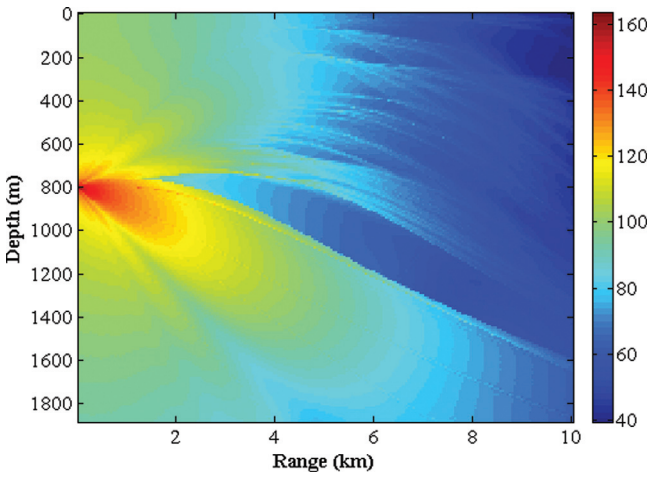

FIG. 2. (Color online) Predicted two-dimensional received level (dB re 1 μPa rms) for a 200 dB re 1 μPa rms SL *M. densirostris* at 800 m depth and −2.5° pitch. This figure was generated using a two-dimensional eigenray propagation model and environmental data.

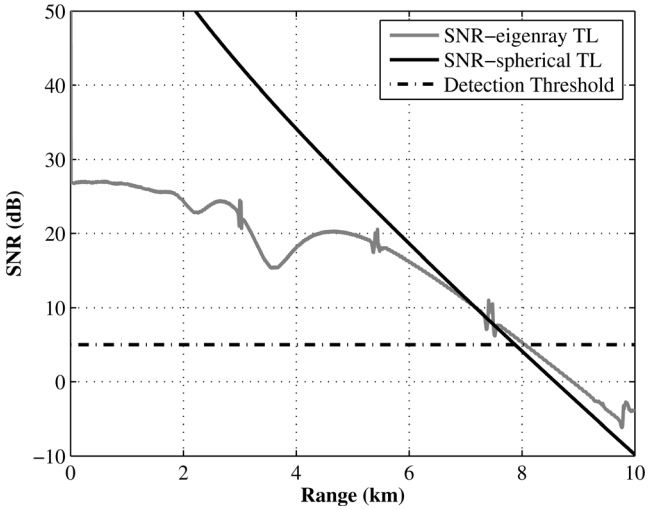

FIG. 4. Predicted SNR as a function of distance for a *M. densirostris* click received at a deep-water bottom-mounted hydrophone (source depth = 800 m, receiver depth = 1630 m, 2.5° pitch angle).

to waves breaking on the reef to the west of this hydrophone. The mean ambient NL as a function of wind speed was estimated by combining the data from hydrophones A and B (Fig. 3, bottom). The correlation between increased wind speed and increased ambient NL is evident. The low- to mid-frequency component of the measured noise spectrum is less than the NL predicted by Eqs. (4) through (7), perhaps due to the acoustically quiet, enclosed nature of the site and deep-water depth of the hydrophones. These equations are based on open ocean measurements that provide only a rough estimate of ambient NL. The high frequency (>22 kHz) measured ambient noise power spectrum is greater than the predicted NLs due to the electronic noise floor of the hydrophones (Fig. 3).

C. GLM fit of baseline and simulated noise *Pd*

Despite the narrow beam width of *M. densirostris*, there is sufficient energy in the off-axis clicks ($n = 10581$) to have a 0.30 *Pd* at 2300 m range (Fig. 5). On-axis clicks ($n = 259$) are detected at ranges of up to 5500 m but there is significantly more scatter in the data at this range due to the small sample size. At baseline ambient NLs (approximately sea-state 1) with no added noise, the GLM fit of the on-axis *Pd* varies from 0.80 at 1000 m range to 0.25 at 6000 m range (Fig. 5). As expected, the *Pd* decreased with increasing simulated NL. With the addition of noise simulating a 10.8 m/s wind speed, the GLM fit of the on-axis *Pd* is reduced to 0.05 at 6000 m range. The GLM fit of off-axis *Pd* has a maximum value of 0.58, decreasing rapidly to 0.03 at 6000 m range. In contrast to the on-axis *Pd*, the addition of noise has the greatest impact on off-axis *Pd* at smaller ranges (Fig. 6). At 1000 m range, the GLM fit of off-axis *Pd* is reduced from a baseline value of 0.58, to 0.34 with the addition of noise simulating a 5.7 m/s wind speed and to 0.32 at 10.8 m/s wind speed.

The GLM fit of *Pd* as a function of SNR, for on-axis and off-axis data combined, is shown in Fig. 7. The GLM predicts a minimum *Pd* of 0.20 at 0 dB SNR and 1.0 at greater than 45 dB SNR. However, at SNRs greater than 30 dB the measured data deviates from the model, suggesting that an unmodeled process may be affecting the results. A comparison of the measured on-axis SNR for baseline clicks (i.e., without added noise) with the predicted SNR obtained earlier using the spherical spreading propagation model is shown in Fig. 8. The theoretical model over-estimates the SNR by at least 5 dB at all ranges and so predicts greater detection ranges than are likely obtainable.

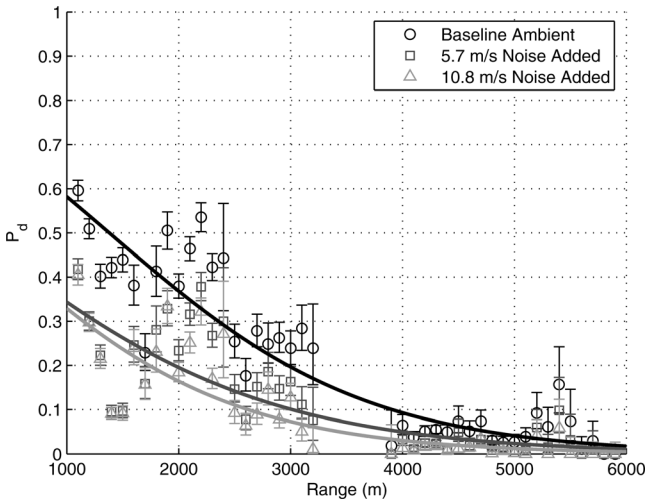

FIG. 6. Empirical *Pd* as a function of slant range for *M. densirostris* off-axis clicks. Measured *Pd* in 500 m range bins, with error bars indicating 95% confidence levels. Solid lines indicate GLM fit for each wind speed.

IV. DISCUSSION

The efficacy of *M. densirostris* passive acoustic detection by widely spaced, bottom-mounted hydrophones is a topic of interest due to monitoring requirements on Navy ranges. While some estimates of acoustic detection probability for beaked whales have been published (Zimmer *et al.*, 2008), an assessment of *M. densirostris* probability of detection has not been previously addressed. Zimmer *et al.* (2008) predicted a 4 km maximum detection range for clicks from a different

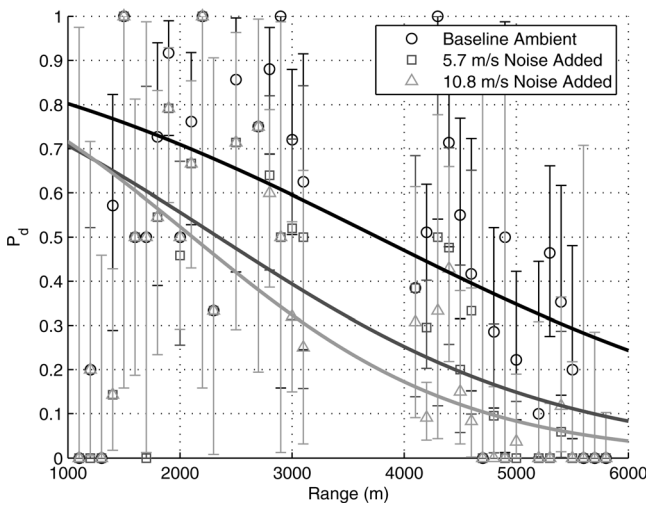

FIG. 5. Empirical *Pd* as a function of slant range for *M. densirostris* on-axis clicks. Measured *Pd* in 500 m range bins, with error bars indicating 95% confidence levels. Solid lines indicate GLM fit for each wind speed.

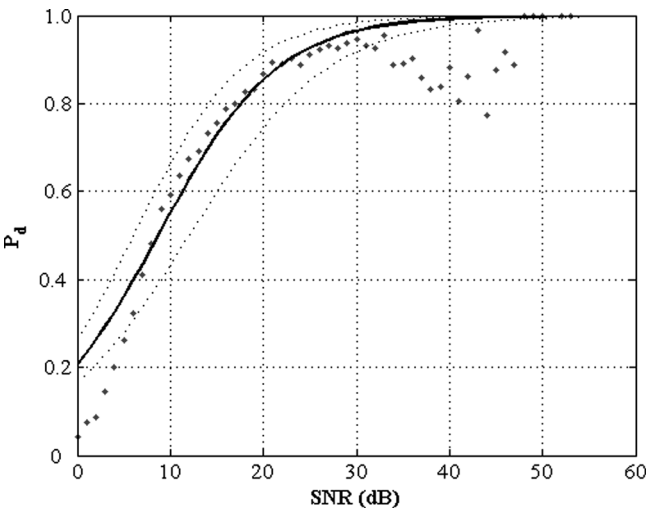

FIG. 7. *Pd* versus SNR for all clicks detected in the baseline ambient data and with added ambient noise (gray points). Solid line is a logistic model fit; dashed lines indicate 95% confidence limits obtained by bootstrap.

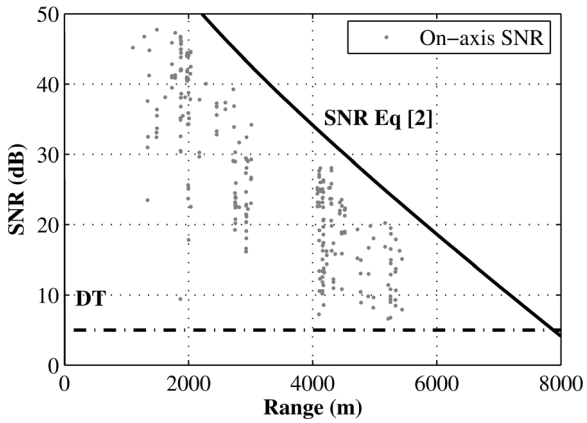

FIG. 8. Measured SNR for all on-axis clicks versus modeled SNR for on-axis clicks as a function of slant range.

beaked whale species, *Z. cavirostris*, received at a near-surface hydrophone assuming spherical spreading, absorption at 40 kHz, and a 30 dB re 1 μPa/$\sqrt{\text{Hz}}$ spectral NL. These assumptions are not applicable to our study due to the deep-water, bottom-mounted hydrophones used at the AUTEC, the unusually low levels of ambient noise at AUTEC, and the lower centroid frequency of *M. densirostris* clicks. *M. densirostris* detection ranges of up to 6500 m have been previously reported for the AUTEC deep-water hydrophones using a matched filter detector (Ward *et al.*, 2008b). The location of the AUTEC facility was originally chosen because of the acoustically quiet nature of the TOTO, which is essentially a deep-water basin isolated by the surrounding islands. The primary source of ambient noise at AUTEC is surface-generated noise such as that caused by increasing wind/wave action and rain (Kurahashi and Gratta, 2008). The ambient NL varies considerably based on the environment, vessel traffic, and surface wind speed. Characteristics of the sensors also affect measured levels of noise. High-frequency sound has greater absorption in seawater and therefore rapidly attenuates for the deep-water hydrophones at AUTEC.

The case study presented here involves results that are specific to the hydrophones and signal processing hardware and software used by the M3R program at the AUTEC facility but the study provides a paradigm for assessing detectability in other settings. Measured NLs were found to vary from levels predicted by the surface noise model in Eqs. (4)–(7). This model includes the directivity of the hydrophones at higher frequencies, the influence of thermal noise and the absorption of high-frequency noise components at the depth of the hydrophones. Nonetheless, the model predicts a noisier environment at low- to mid-frequencies than measurements indicate. This difference may be a result of the empirical nature of the ambient noise models which are based on open ocean data from a noisier environment. Past studies of the AUTEC ambient noise environment indicate that the Knudsen curves accurately predict the shape of ambient noise below 15 kHz but not at higher frequencies (Kurahashi and Gratta, 2008). At higher frequencies, the measured ambient NL is limited by the electronic noise floor of the hydrophones, thus models would predict a lower NL than actually measured. System noise also tends to limit the effect of wind speed variation on the high-frequency ambient NL. For example, at 15 kHz there is a 20 dB spread between the maximum and minimum observed NL, while at 30 kHz the spread is only 8 dB, and by 40 kHz the spread has decreased to 4 dB (Fig. 3, hydrophone B). Although wind speed was correlated with the measured ambient levels, the correlation was not strong presumably owing to the 21 km distance between the weather station and measurement hydrophones providing ample scope for wind direction and speed changes (Kurahashi and Gratta, 2008).

The results of this study emphasize the need for *in-situ* measurements of ambient and system noise, and a thorough understanding of the hydrophone response sensitivity for accurate predictions of acoustic detection probability. High-frequency surface-generated noise arrives from above, where the receiver sensitivity of the AUTEC hydrophones is reduced at high frequencies. However, *M. densirostris* sound emissions at depths of 700–900 m are more often received at angles of greater hydrophone response sensitivity, improving the SNR of the received clicks. The 20 dB spread found in on-axis SNR (Fig. 8) is caused by changes in SL as well as NL. Apparent variation in on-axis SLs may relate to click-to-click SL variability previously noted in *M. densirostris* foraging click apparent output levels (Madsen *et al.*, 2005) and may also result from uncertainty as to the pointing direction of the sound source due to the posterior position of the tag on the whale.

Previous analysis of the M3R FFT detector indicated a maximum 0.80 *Pd* at 25 dB SNR in the presence of Gaussian white noise (Ward *et al.*, 2008b). While typically *Pd* is expected to approach unity at high SNR, the detector's lower performance is likely linked to the choice of time constant in the exponential noise filter (Ward *et al.*, 2008b). A short time constant will lead to fluctuations in the detection threshold when high-level transients such as high SNR clicks are received. This may account for the scatter observed below the GLM fit in Fig. 7 for measurements above 30 dB SNR.

Deep-water hydrophone ranges provide an excellent opportunity for passive acoustic monitoring of *M. densirostris* due to the attenuation of high-frequency surface-generated ambient noise at depth and the resulting higher SNR of received clicks for a given range as compared to shallow hydrophones. Given the empirical *Pd* curves (Figs. 5 and 6), one would expect to be able to detect a single click on more than one hydrophone if the hydrophones are sufficiently closely spaced, an important capability for passive acoustic localization. Off-axis *Pd* is reduced to less than 0.2 to at ranges greater than 3000 m, adversely affecting the ability to localize animals during increased sea-state. However, this would not interfere with mitigation measures that simply require knowledge of species presence or absence. While on-axis *Pd* decreases significantly with increasing ambient noise, the *Pd* is still above 0.10 at 5500 m range for the worst wind conditions modeled. At this *Pd*, and given the large number of clicks emitted per dive, the animal is very likely to be detected if present. This is in significant contrast to the effect of increasing sea-state on visual observations of *M. densirostris*, which can experience a ten-fold reduction in encounter rates between Beaufort 0–1 and Beaufort 5 sea-states (Barlow, 2006; Schorr *et al.*, 2009).

In providing estimates of *M. densirostris Pd* and detection range, careful attention needs to be made to accurately represent the surrounding acoustic environment. For bottom-mounted, deep-water hydrophones, the effects of high-frequency sound absorption as surface-generated noise propagates to the deep sensors are particularly important as both the TL and ambient noise (NL) are impacted. The theoretical model developed here predicted a detection range of approximately 7800 m while the empirical results showed a 5500 m maximum detection range. However, only 1% of the clicks available in the study were beyond 5500 m range and none exceeded 6000 m. Additional data from DTag deployments on *M. densirostris* during the BRS2007 experiment, not used in this study, indicated a 6500 m maximum detection range for the same FFT detector (Marques *et al.*, 2009). The *Pd* results obtained in this study cannot be directly compared to Marques *et al.* (2009) as the current study did not include the effects of a classifier. Data from hydrophones at greater ranges need to be evaluated to determine the maximum detection range of *M. densirostris* as a function of SNR. This would provide regulators and environmental managers with an accurate estimate of how *M. densirostris Pd* varies with respect to sea-state conditions over the entire potential detection range.

ACKNOWLEDGMENTS

These data were collected during the 2007 Behavioral Response Study (BRS) funded by N45, Office of Naval Research, Integrated Warfare Systems 5 (IWS5) and Strategic Environmental Research and Development Program. We would like to thank the entire field team that participated in the 2007 BRS for supporting the effort that provided the data used in this study. This work was funded by two partners under the National Oceanographic Partnership Program: The Ocean Acoustics Program of the U.S. National Marine Fisheries Service, Office of Protected Resources, and the International Association of Oil and Gas Producers Joint Industry Programme on Exploration and Production Sound and Marine Life. The research permits were issued to John Boreman (U.S. National Marine Fisheries Service (NMFS) 1121-1900), Peter Tyack (U.S. NMFS 981-1578), and Ian Boyd (Bahamas permit #02/07). The tagging research was approved by the WHOI Institutional Animal Care and Use Committee. In addition, this work would not have been possible without the contributions of David Deveau, who provided the historical ambient noise measurements, and the late Jim Pazera, who generously shared his expertise as system engineer of the AUTEC hydrophones shortly before his untimely death. Jim is greatly missed by all his colleagues at NUWC.

Barlow, J. (**2006**). "Cetacean abundance in Hawaiian waters estimated from a summer/fall survey in 2002," Marine Mammal Sci. **22**, 446–464.

Boyd, I. L., Claridge, D. E., Clark, C. W., Southall, B. L., and Tyack, P. L. (**2007**). Behavioral Response Study Cruise Report (BRS-2007), available at www.nmfs.noaa.gov/pr/pdfs/acoustics/brs07_report.pdf.

Jarvis, S. (**1993**). Signature Simulation (SigSim) System: Development and Capabilities, NUWC-NPT Technical Report 10,224 (UNCLASSIFIED), Naval Undersea Warfare Center, Newport, Rhode Island.

Johnson, M., Aguilar de Soto, N., Madsen, P. T. (**2009**). "Studying the behaviour and sensory ecology of marine mammals using acoustic recording tags: A review," Mar. Ecol.: Prog. Ser. **395**, 55–73.

Johnson, M. P., Madsen, P. T., Zimmer, W. M. X., Aguilar de Soto, N., and Tyack, P. L. (**2004**). "Beaked whales echolocate on prey," Proc. R. Soc. London, Ser. B **271**, S383–S386.

Johnson, M., Madsen, P. T., Zimmer, W. M. X., Aguilar de Soto, N., and Tyack, P. L. (**2006**). "Foraging Blainville's beaked whales (*Mesoplodon densirostris*) produce distinct click types matched to difference phases of echolocation," J. Exp. Biol. **209**, 5038–5050.

Johnson, M. P., and Tyack, P. L. (**2003**). "A digital acoustic recording tag for measuring the response of wild marine mammals to sound," IEEE J. Ocean. Eng. **28**, 3–12.

Kurahashi, N., and Gratta, G. (**2008**). "Oceanic ambient noise as a background to acoustic neutrino detection," Phys. Rev. D **78**, 1–5.

Lurton, X. (**2002**). An introduction to underwater acoustics: Principles and applications (Praxis Publishing, U.K.).

Madsen, P. T., Johnson, M., Aguilar deSoto, N., Zimmer, W. M. X., and Tyack, P. (**2005**). "Biosonar performance of foraging beaked whales (*Mesoplodon densirostris*)," J. Exp. Biol. **208**, 181–194.

Madsen, P. T., and Wahlberg, M. (**2007**). "Recording and quantification of ultrasonic echolocation clicks from free-ranging toothed whales," Deep-Sea Res. **54**, 1421–1444.

Maripro, Incorporated (**2002**). Atlantic Undersea Test and Evaluation Center (AUTEC) Hydrophone Replacement Program (AHRP) Training Materials/Training Program, Contract No. N66604-97-C-0347.

Marques, T. A., Thomas, L., Ward, J., DiMarzio, N., and Tyack, P. (**2009**). "Estimating cetacean population density using fixed passive acoustic sensors: An example with beaked whales," J. Acoust. Soc. Am. **125**, 1982–1994.

McCullagh, P., and Nelder, J. A. (**1997**). *Generalized Linear Models* (Chapman and Hall/CRC, New York), 511 p.

Moretti, D., DiMarzio, N., Morrissey, R., Ward, J., and Jarvis, S. (**2006**). "Estimating the density of Blainville's beaked whale (*Mesoplodon densirostris*) in the Tongue of the Ocean (TOTO) using passive acoustics," in *Proceedings of IEEE OCEANS 2006 Conference*, Boston, MA, pp. 1–5.

Morrissey, R. P., Ward, J., DiMarzio, N., Jarvis, S., and Moretti, D. J. (**2006**). "Passive acoustic detection and localization of sperm whales (*Physeter macrocephalus*) in the Tongue of the Ocean," Appl. Acoust. **67**, 1091–1105.

Rasmussen, M. H., Wahlberg, M., and Miller, L. A. (**2004**). "Estimated transmission beam pattern of clicks recorded from free-ranging white-beaked dolphins (*Lagenorhynchus albirostris*)," J. Acoust. Soc. Am. **116**, 1826–1831.

Schorr, G. S., Baird, R. W., Hanson, M. B., Webster, D. L., McSweeney, D. J., and Andrews, R. D. (**2009**). "Movements of satellite-tagged Blainville's beaked whales off the island of Hawai'i," Endang. Species Res. **10**, 203–213.

Short, J. R. (**2005**). "High-frequency ambient noise and its impact on underwater ranges," J. Ocean. Eng. **30**, 267–274.

Tyack, P. L., Johnson, M. P., Zimmer, W. M. X., Aguilar de Soto, N., and Madsen, P. T. (**2006a**). "Acoustic behavior of beaked whales, with implications for acoustic monitoring," in *Proceedings of IEEE Oceans 2006 Conference*, Boston, MA, pp. 1–6.

Tyack, P. L., Johnson, M. P., Aguilar de Soto, N., Sturlese, A., and Madsen, P. T. (**2006b**). "Extreme diving behaviour of beaked whale species known to strand in conjunction with use of military sonars," J. Exp. Biol. **209**, 4238–4253.

Ward, J. A. (**2002**). Sperm Whale Bioacoustic Characterization in the Tongue of the Ocean, Bahamas, NUWC-NPT TR 11,398 (Naval Undersea Warfare Center, Division Newport, RI), September 20, 2002.

Ward, J., Moretti, D., Morrissey, R. P., DiMarzio, N. A., Tyack, P., and Johnson, M. (**2008a**). "*Mesoplodon densirostris* transmission beam pattern estimated from passive acoustic bottom mounted hydrophones and a DTag record," J. Acoust. Soc. Am. **123**, 3619.

Ward, J., Morrissey, R., Moretti, D., DiMarzio, N., Jarvis, S., Johnson, M., Tyack, P., and White, C. (**2008b**). "Passive acoustic detection and localization of *Mesoplodon densirostris* (Blainville's beaked whale) sound emissions using distributed bottom-mounted hydrophones in conjunction with a digital tag recording," Can. Acoust. **36**, 60–66.

Weinberg, H., and Keenan, R. (**1996**). "Gaussian ray bundles for modeling high-frequency propagation loss under shallow-water conditions," J. Acoust. Soc. Am. **100**, 1421–1431.

Zimmer, W. M. X., Harwood, J., Tyack, P., Johnson, M., and Madsen, P. (**2008**). "Passive acoustic detection of deep-diving beaked whales," J. Acoust. Soc. Am. **124**, 2823–2832.

Zimmer, W. M. X., Johnson, M. P., Madsen, P. T., and Tyack, P. L. (**2005a**). "Echolocation clicks of free-ranging Cuvier's beaked whales (*Ziphius cavirostris*)," J. Acoust. Soc. Am. **117**, 3919–3927.

Zimmer, W. M. X., Madsen, P. T. M., Teloni, V., Johnson, M., and Tyack, P. L. (**2005b**). "Off-axis effects on the multi-pulse structure of sperm whale usual clicks with implications for the sound production," J. Acoust. Soc. Am. **118**, 3337–3345.